INTERNATIONAL JOURNAL OF PRECISION ENGINEERING AND MANUFACTURING-GREEN TECHNOLOGY Vol. 4, No. 1, pp. 73-78 JANUARY 2017 | 73
DOI: 10.1007/s40684-017-0010-5 ISSN 2288-6206 (Print) | ISSN 2198-0810 (Online)

Both Energy and Cost-Effective Semi-Active RFC (Reaction Force Compensation) Method for Linear Motor Motion Stage

Kim Duc Hoang[1] and Hyeong-Joon Ahn[2,#]

1 Department of Software Convergence, Graduate School, Soongsil University, 369, Sangdo-ro, Dongjak-gu, Seoul, 06978, South Korea
2 Department of Mechanical Engineering, Soongsil University, 369, Sangdo-ro, Dongjak-gu, Seoul, 06978, South Korea
Corresponding Author | Email: ahj123@ssu.ac.kr, TEL: +82-2-820-0654., FAX: +82-2-820-0668

KEYWORDS: Linear motor motion stage, Residual vibration, Semi-Active reaction force compensation (RFC), Switching an extra coil

Residual vibration of the system base due to the rapid acceleration of a motion stage may significantly reduce life span and productivity of the manufacturing equipment. Although a passive reaction force compensation (RFC) mechanism was developed to reduce the residual vibration of a linear motor motion stage, the passive RFC cannot adjust its dynamic characteristic against the motion profile variation. An active RFC mechanism using an additional coil can tune spring and damping of the RFC system according to the motion profile of the mover, but both cost and energy consumption of the active RFC are very high and it is not suitable for green manufacturing. In this paper, we develop a semi-active RFC method by switching an extra coil for a linear motor motion stage to tune damping of the RFC system against the motion profile variations. First, we investigate the effect of switching the extra coil with free vibration test of the magnet track, which shows that the damping of the RFC can be adjusted by the open-close ratio of the extra coil. In addition, two kinds of motion profiles such as long and short stroke motions are used to confirm the semi-active RFC by switching the extra coil. The effectiveness of the semi-active RFC method was verified with simulations and experiments.

Manuscript Received: July 1, 2016 | Revised: November 4, 2016 | Accepted: November 9, 2016

NOMENCLATURE

k_{MT} = Stiffness of magnet track
c_{MT} = Damping of magnet track
m_{MT} = Mass of magnet track
a,b,c = a-b-c three phase coordinate
i_a,i_b,i_c = Three phase currents in a-b-c frame
I_d,I_q = Currents in d-q frame
e_{an},e_{bn},e_{cn} = Back-EMF of extra coil
R_{coil} = Resistance of extra coil
L_{coil} = Inductance of extra coil
R_{load} = Load resistance
R_q^{coil} = Resistor of coil in q-axis
L_q^{coil} = Inductance of extra coil in q-axis
R_q^{load} = Resistance load in q-axis
r_{OC} = Open-close time ratio
e_q^{coil} = Back-EMF in q-axis
c_{coil} = Damping coefficient of extra coil
F_t = Thrust force of mover
F_{coil} = Lorentz force of extra coil
F_{trans} = Transmitted force
p = Number of pole pairs
τ = Magnet track pole pitch
ψ = Flux linkage of magnet track
K_{emf} = Electromotive force gain
K_f = Force constant of extra coil

1. Introduction

High-speed and ultra-precision positioning devices are widely used to manufacture flat panel displays and semiconductors. The mechanical structural technologies, as well as advanced control technologies are

© KSPE and Springer 2017

being investigated due to increasing demands for improved productivity. In detail, a motion stage for 450 mm wafer has performance of 5 g acceleration, accuracy 50 nm, resolution 0.1 nm.[1-3]

Rapid acceleration or deceleration motion of a mover transfers a large reaction force to its system base so that the system base may vibrate either with large amplitude or extended settling time. In consequence, high-speed motion causes the residual vibration of its system base and may reduce life span and productivity of the manufacturing device although higher acceleration motion is required to improve the production throughput.

There are three main approaches to reduce the residual vibration of a mechanical system. The first method is to adjust the motion input to excite the vibration such as input shaping.[4] The second method is to use an advanced control algorithm or additional feedback controller to suppress the vibration of the system.[5] The last one is to introduce special kinematic structure for fundamental avoidance of the excitation source like force balancing.[6]

Kind of the last approach or a passive RFC for a linear motor motion stage can reduce the system vibration with a movable magnet track, spring and damper.[7-9] The passive RFC mechanism is compact and cost-effective without any additional external structures or actuator. However, the passive RFC doesn't allow in-situ modification of the dynamic characteristic and may have resonance when a motion profile excites natural frequency of the RFC mechanism. An active RFC mechanism using an additional coil can tune its stiffness of the magnet track, and minimize the transmitted force under motion profile variations.[10] However, the active RFC mechanism results in increasing energy and cost requirements due to extra servo amplifier and motion controller, which is not suitable for green manufacturing.[11,12]

Active characteristic without increasing energy consumption could be achieved using motors. A linear motor was utilized as a variable damper by changing an additional resistance connected to the coil.[13] The variable damper system using a motor does not consume any energy, but harvests the vibration energy.[14] Although a semi-active RFC mechanism by changing resistor was introduced,[15] there is limitation to adjust the resistance in-situ.

This paper presents a both energy and cost-effective semi-active RFC method for a linear motor motion stage. The semi-active RFC by switching an extra coil can reduce power consumption and complexity of the system compared with the fully active RFC. A three-phase circuit model of the semi-active RFC is derived and its simulation model is built. Typical two motion profiles are introduced to verify its adjustable damping capability by switching the extra coil. Finally, we verify effectiveness of the semi-active RFC mechanism with both simulations and experiments.

2. Semi-Active RFC

2.1 Principle

Schematic diagrams of the passive and the semi-active RFC mechanisms for a linear motor system are compared in Fig. 1. The passive RFC comprises a movable magnet track, spring and damper, as shown in Fig. 1(a) and we cannot adjust in-situ its dynamic characteristic against the motion profile variations although the transmitted force to the system base is reduced. On the other hand, the proposed semi-active RFC of this paper has an extra coil with a switch,

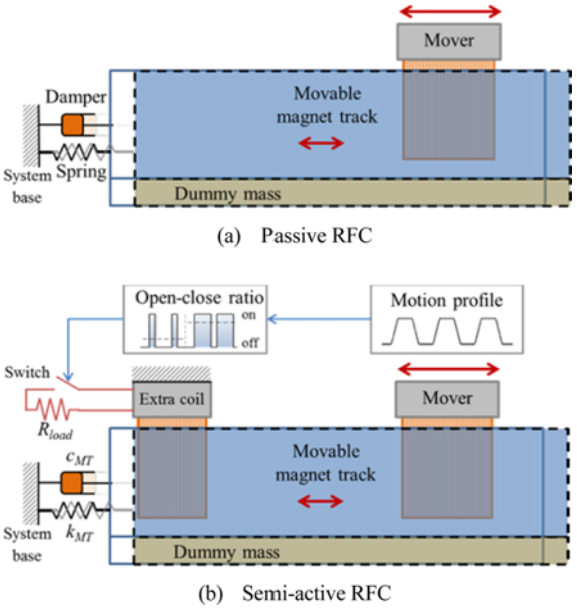

Fig. 1 Schematic diagram of the semi-active RFC mechanism

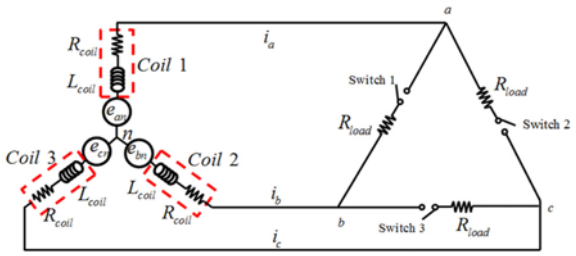

Fig. 2 Three-Phase circuit of the extra coil and switch

as shown in Fig. 1(b). When the mover moves following a motion profile, the magnet track oscillates with supporting of spring k_{MT} and damper c_{MT} like the passive RFC, which induces current of the extra coil proportional to the speed of the magnet track. The current due to the magnet track oscillation generates the electromotive force of the extra coil by interacting with the magnet track, when the extra coil is closed by the switch. That is, the extra coil generates damping force from the kinetic energy of the magnet track without any external energy, which reduces the energy consumption significantly compared with the active RFC.[10] In addition, damping of the extra coil can be adjusted by changing open-close time ratio of the extra coil without any additional servo amplifier and motion control axis so that the system complexity is reduced.

2.2 Model of the Semi-Active RFC

2.1.1 Equation of Motion of Three Phase Circuit

A schematic diagram of the three-phase circuit model for the semi-active RFC is shown in Fig. 2.[15] A coreless type linear motor mover coil of wye connection is used for the extra coil, and a switch and a resistor are serially connected to each phase using delta connection.

Assuming that the three-phase circuit is well balanced, DQ transformation converts the three-phase circuit of the semi-active RFC into an equivalent circuit in q-axis, as shown in Fig. 3. Here, R_q^{coil} is the resistor of the extra coil in q-axis, L_q^{coil} is the inductance of the extra coil in q-axis, R_q^{load} is the resistance load of the circuit in q-axis and e_q^{coil} is the electromotive force of the extra coil due to the magnet track motion.

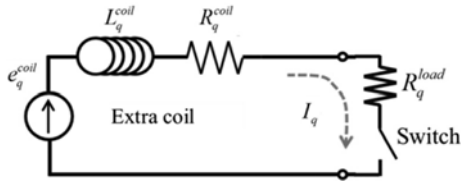

Fig. 3 An equivalent circuit diagram of the extra coil in q-axis

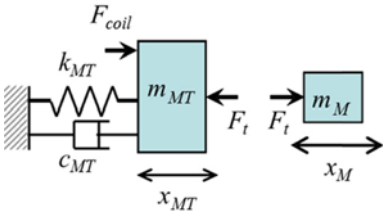

Fig. 4 A schematic diagram of the semi-active RFC in mechanical domain[7]

When the switch is closed, the circuit equation of the extra coil can be and load resistor can be expressed as Eq. (1). In addition, the equivalent resistor in q-axis are shown in Eq. (2). Here, I_q is the equivalent current in q-axis.

$$e_q^{coil} = R_q^{coil} I_q + L_q^{coil} \frac{dI_q}{dt} + R_q^{load} I_q \tag{1}$$

$$R_q^{coil} = R_{coil} \text{ and } R_q^{load} = R_{load} \tag{2}$$

2.1.2 Equation of Motion of the Magnet Track

Fig. 4 shows a schematic diagram of the semi-active RFC in mechanical domain. 1-DOF dynamic equation of the magnet track motion and the transmitted force to the system base are expressed as Eqs. (3) and (4), respectively.

$$m_{MT}\ddot{x}_{MT} + c_{MT}\dot{x}_{MT} + k_{MT}x_{MT} = -F_t + F_{coil} \tag{3}$$

$$F_{tran} = c_{MT}\dot{x}_{MT} + k_{MT}x_{MT} + F_{coil} \tag{4}$$

where, m_{MT} is the mass of the magnet track, x_{MT}, $\dot{x}_{MT}$ and $\ddot{x}_{MT}$ are position, velocity and acceleration of the magnet track, respectively.

2.1.3 Electromechanical System

The magnet track motion induces electromotive force of the extra coil according to Faraday's law. Assuming that time constant of the extra coil and the load resistor is much smaller than the switching period, Lorentz force generated by the induced current of the extra coil and the magnetic flux of the magnet track is calculated by Eq. (5).

$$F_{coil} = \frac{3}{2} p \frac{\pi}{\tau} (\psi + (L_d^{coil} - L_q^{coil}) I_d) r_{OC} I_q \tag{5}$$

where, ψ is the flux linkage of the magnet track, L_d and L_q are the d-axis and q-axis inductances, p is the number of pole pairs, r_{OC} is open-close time ratio (r_{OC} = 0: fully open and r_{OC} = 1: fully close), I_d and I_q are the currents of the extra coil in d and q-axis, respectively.

Due to low inductance of the extra coil, we can approximate the Lorentz force of the extra coil as Eq. (6). In addition, we can express the electromotive force of the extra coil in q-axis as Eq. (7). Here, K_f is motor current gain and e_q^{coil} is the electromotive force of the extra coil in q-axis.

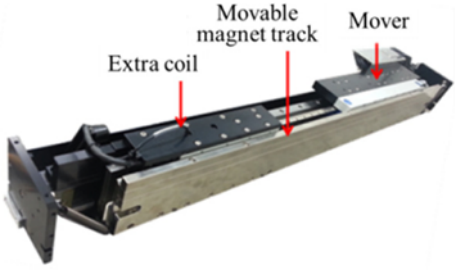

(a) The linear motor motion stage

(b) Extra coil with hall sensors

Fig. 5 Experimental set-up

$$F_{coil} \approx r_{OC} \frac{3}{2} p \frac{\pi}{\tau} \psi I_q = r_{OC} K_f I_q \tag{6}$$

$$e_q^{coil} = K_{emf} \dot{x}_{MT} \tag{7}$$

Using Eqs. (1), (6) and (7), we can derive the transfer function from $F_{coil}(s)$ to $sX_{MT}(s)$, as shown in Eq. (8).

$$\frac{F_{coil}(s)}{sX_{MT}(x)} = \frac{r_{OC} K_f K_{emf}}{R_q^{coil} + R_q^{load} + sL_q^{coil}} \tag{8}$$

Considering the low frequency oscillation of the magnet track and the low inductance L_q^{coil}, we can derive an approximate transfer function from the velocity of the magnet track as Eq. (9). The damping coefficient of the extra coil can be adjusted with r_{OC} or open-close time ratio.

$$c_{coil} = \frac{F_{coil}(s)}{sX_{MT}} \approx \frac{r_{OC} K_f K_{emf}}{R_q^{coil} + R_q^{load}} \tag{9}$$

where, c_{coil} is the damping coefficient of the extra coil.

2.3 Design Considerations

Maximum damping from the extra coil can be adjusted with the load resistors, as shown in Eq. (9). With given motion profiles, we can calculate corresponding transmitted forces and magnet track motions. Then, we determine a desired damping for each motion profile.

The load resistor decreases the time constant of the extra coil and improves the damping adjustment capability of damping adjustment of the semi-active RFC. Switching period of the extra coil should be much smaller than the natural frequency of the magnet track for effective damping control.

3. Simulations and Experiments

3.1 Experimental Set-Up and Simulation Model

Fig. 5 shows a photo of the linear motor motion stage with the extra coil. The mover moves along the linear guide interacting with the movable magnet track. The extra coil is installed on the system base to

Table 1 System parameters of the linear motor motion stage

Parameter	Value	Parameter	Value
m_{MT}	21 kg	K_{emf}	20 Vs/m
k_{MT}	155 N/m	R_{coil}	1.7 Ω
m_M	5 kg	L_{coil}	0.002 H
K_f	20 N/A	R_{load}	1.5 Ω
c_{MT}	20Ns/m	Period	100ms

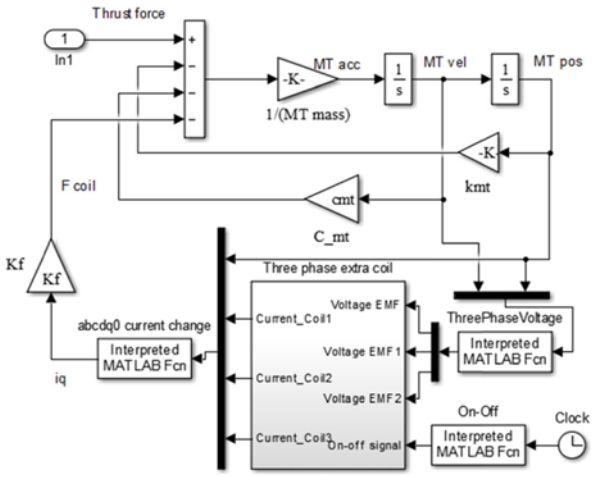

(a) A simulink model for the linear motor motion stage with the semi-active RFC

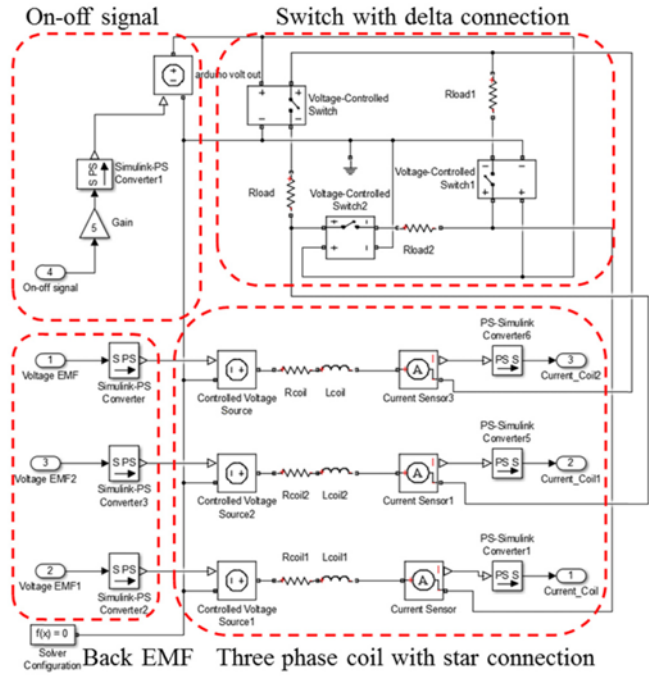

(b) Three-Phase circuit model of the extra coil

Fig. 6 A simulation model of the semi-active RFC

adjust damping of the magnet track and hall sensors are installed in the extra coil to measure the magnet track motion for commutation.[16,17] The extra coil is serially connected to both a set of relay switches (G6L-1P DC5) and external resistors in the delta connection. The relay is controlled by an Arduino board. Specifications of the linear motor motion stage are as follows: max thrust force 810 N (continuous 240 N), 1 μm resolution, 380 mm stroke (510 mm without the semi-active coil), max speed 5.0 m/s and max acceleration 35 m/s^2 and peak

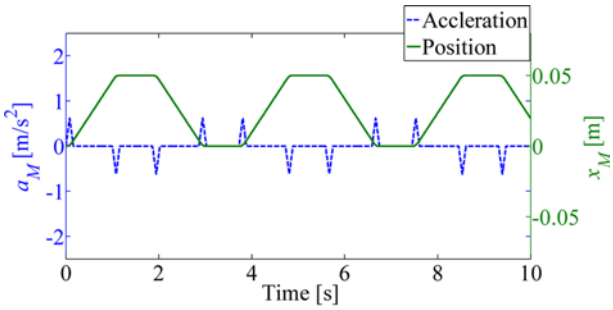

(a) Long stroke motion

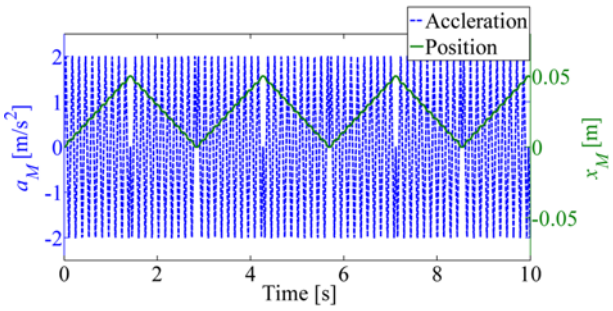

(b) Short stroke motion

Fig. 7 Motion profiles for simulation and experiment

current of the extra coil 6 A. Therefore, max damping force of the extra coil is about 120 N and max damping coefficient of the extra coil is about 160 Ns/m (with a resistor 1.5 Ω).

We build a simulation model consisting of both electrical (Fig. 2) and mechanical (Fig. 4) systems using sim-scape,[18] as shown in Fig. 6. In particular, the simulation model includes a full three-phase circuit model (wye-connected three-phase coils with delta-connected switches), such as wye connected three phase coils with delta connected switches, as shown in Fig. 6(b). Parameters for the linear motor motion stage with the semi-active RFC are shown in Table 1. Most parameters are identified from the experimental set-up.[9]

Two motion profiles for simulation and experiment: long and short stroke motions are shown in Fig 7. First one is the long stroke motion: The peak acceleration is 0.6 m/s^2, the peak velocity is 0.9 m/s and the stroke is 0.35 m, respectively. The other one is the short stroke motion: The peak acceleration is 2 m/s^2, the peak velocity is 0.9 m/s and the stroke is 0.05 m, respectively.

3.2 Results

In order to verify feasibility of the semi-active RFC, free vibration tests of the magnet track with various open-close time ratios (from 0% to 100% by 20%) are performed and shown in Fig. 8(a). During the free vibration tests, we set the period of time 100ms and the magnet track motion is measured with a hall sensor array.[16,17] Then, damping coefficients are evaluated from the logarithmic decrement of the free vibration and shown in Fig. 8(b). Damping of the magnet track is proportional to the on-time ratio of the extra coil.

Fig. 9 compares simulation and experimental magnet track motions for both motion profiles and various on-time ratios. We set the switching period 100 ms and adjust the on-time ratio (0%, 50%, 70%, 100%). As the on-time ratio increases, the damping of the magnet track increases and its peak motion decreases. There are small different

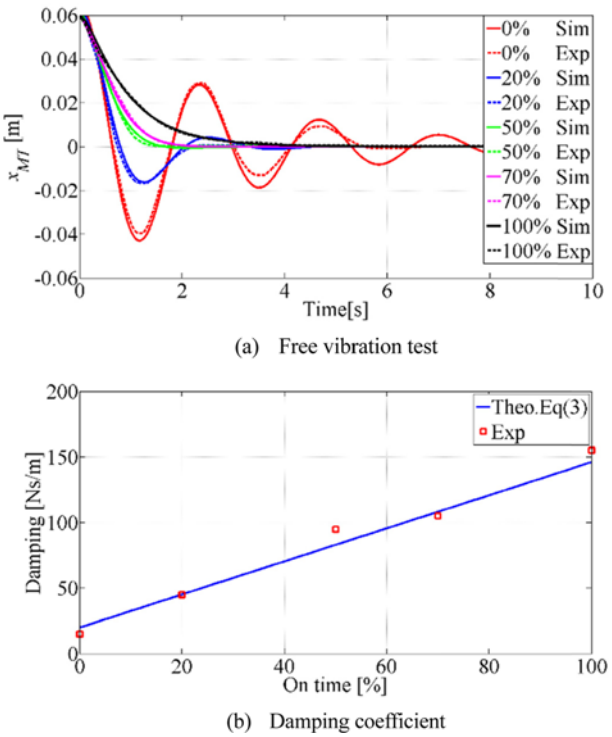

(a) Free vibration test

(b) Damping coefficient

Fig. 8 Free vibration test of the semi-active RFC

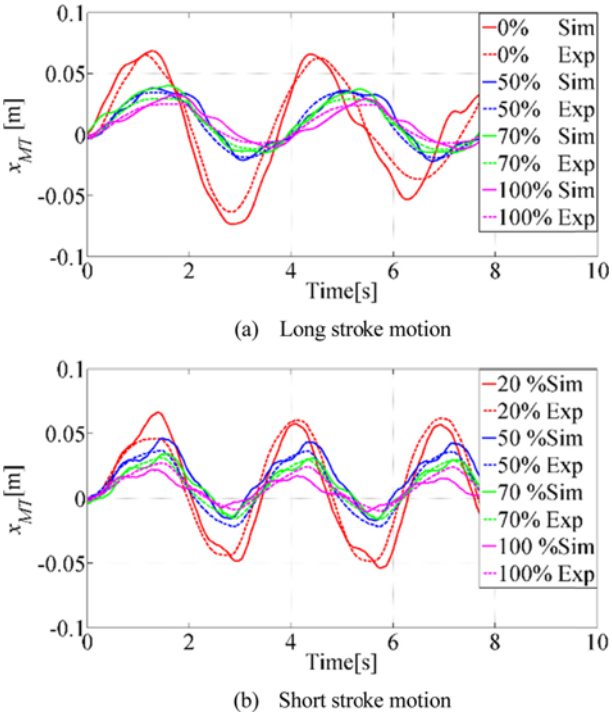

(a) Long stroke motion

(b) Short stroke motion

Fig. 9 magnet track motion with open-close ratio variations

between simulation and experiment, which is caused by an approximate friction model with linear damping coefficient.[19]

Fig. 10 shows measured three phase current (i_a, i_b, i_c) and dq current (i_q, i_d) of the extra coil for both motion profiles. As shown in Fig. 10, i_q is more dominant than i_d to produce the damping force.[15]

Fig. 11 shows the thrust and the transmitted forces for both motion profiles and various on-time ratios. The black-dash lines present the

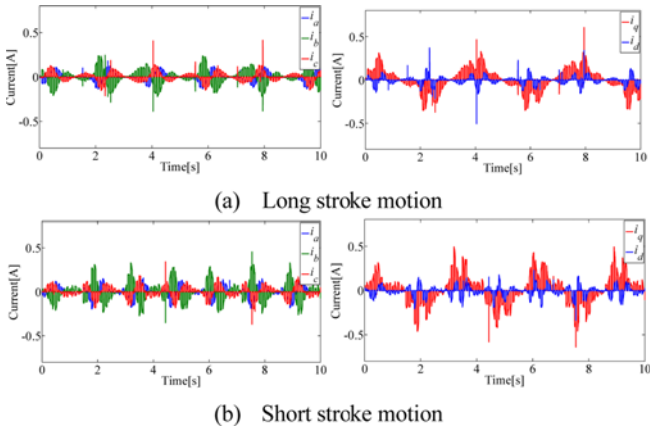

(a) Long stroke motion

(b) Short stroke motion

Fig. 10 Three phase current with 50% on-time ratio

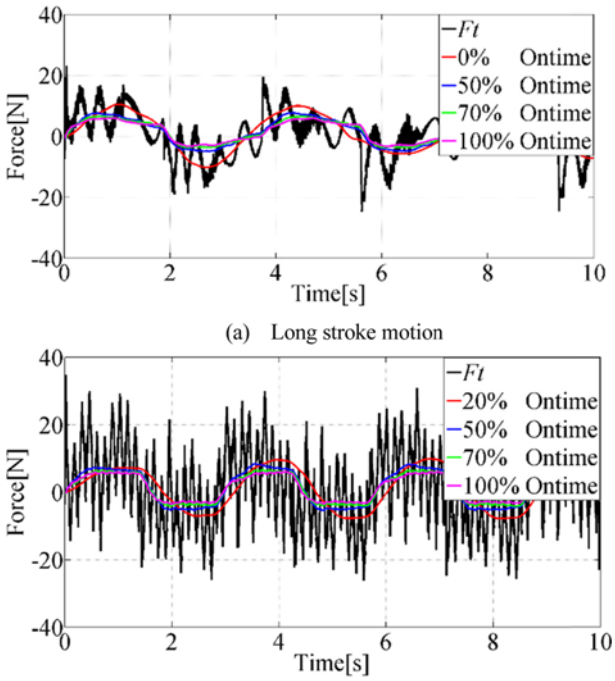

(a) Long stroke motion

(b) Short stroke motion

Fig. 11 Transmitted force and magnet track motion with open-close ratio variations

thrust force while the red, blue, green and purple lines denote the transmitted force to the system base for 20%, 50%, 70% and 100% on-time ratios, correspondingly. We can reduce the transmitted force to the system base by the proposed semi-active RFC, about 40-50% for the long stroke motion and about 50-60% for the short stroke motion.

4. Conclusions

This paper presents a both energy and cost-effective semi-active RFC method for a linear motor motion stage. The semi-active RFC method by switching an extra coil is a kind of green manufacturing technology since it can reduce both power consumption and complexity of the motion system compared to the active RFC. A three-phase circuit model of the semi-active RFC is derived and a simulation

model for the semi-active RFC by switching the extra coil was built. Typical two motion profiles are introduced to verify its adjustable damping capability by switching the extra coil. Finally, effectiveness of the semi-active RFC method is verified with simulations and experiments.

ACKNOWLEDGEMENT

This work was by Basic Science Research Program through the National Research Foundation of Korea (NRF) funded by the Ministry of Education, Science and Technology (NRF-2013R1A1A2010764).

REFERENCES

1. Newport, "DynamYX DATUM Ultra-High Performance Air Bearing Stage, http://www.newport.com/DynamYX-DATUM-Ultra-High-Performance-Stage/646127/1033/info.aspx (Accessed 8 December 2016)
2. Yu, P., Chen, X., Wang, X., and Jiang, W., "Frequency-Dependent Nonlinear Dynamic Stiffness of Aerostatic Bearings Subjected to External Perturbations," Int. J. Precis. Eng. Manuf., Vol. 16, No. 8, pp. 1771-1777, 2015.
3. Woo, S. and Gweon, D.-G., "Design and Optimization of Long Stroke Planar Motion Maglev Stage Using Copper Strip Array," Int. J. Precis. Eng. Manuf., Vol. 16, No. 3, pp. 479-485, 2015.
4. Li, H., Le, M., Gong, Z., and Lin, W., "Motion Profile Design to Reduce Residual Vibration of High-Speed Positioning Stages," IEEE/ASME Transactions On Mechatronics, Vol. 14, No. 2, pp. 264-269, 2009.
5. Iwasaki, M., Seki, K., and Maeda, Y., "High-Precision Motion Control Techniques: A Promising Approach to Improving Motion Performance," IEEE Industrial Electronics Magazine, Vol. 6, No. 1, pp. 32-40, 2012.
6. Arakelian, V. H. and Smith, M., "Shaking Force and Shaking Moment Balancing of Mechanisms: A Historical Review with New Examples," Journal of Mechanical Design, Vol. 127, No. 2, pp. 334-339, 2005.
7. You, Y.-H. and Ahn, H.-J., "A Passive Reaction Force Compensation (RFC) Mechanism for a Linear Motor Motion Stage," Int. J. Precis. Eng. Manuf., Vol. 15, No. 5, pp. 797-801, 2014.
8. Nguyen, D. C. and Ahn, H. J., "Dynamic Analysis and Iterative Design of a Passive Reaction Force Compensation Device for a Linear Motor Motion Stage," Int. J. Precis. Eng. Manuf., Vol. 15, No. 11, pp. 2367-2373, 2014.
9. Ahn, H.-J., "Eddy Current Damper Type Reaction Force Compensation Mechanism for Linear Motor Motion Stage," Int. J. Precis. Eng. Manuf.-Green Tech., Vol. 3, No. 1, pp. 67-74, 2016.
10. Nguyen, D. C. and Ahn, H.-J., "A Fuzzy-P Controller of an Active Reaction Force Compensation (RFC) Mechanism for a Linear Motor Motion Stage," Int. J. Precis. Eng. Manuf., Vol. 16, No. 6, pp. 1067-1074, 2015.
11. Dornfeld, D. A., "Green Manufacturing: Fundamentals and Applications," Springer Science & Business Media, 2012.
12. Diaz, N., Choi, S., Helu, M., Chen, Y., Jayanathan, S., et al., "Machine Tool Design and Operation Strategies for Green Manufacturing," Proc. of 4th CIRP Conference on High Performance Cutting, 2010.
13. Karnopp, D., "Permanent Magnet Linear Motors Used as Variable Mechanical Dampers for Vehicle Suspensions," Vehicle System Dynamics: International Journal of Vehicle Mechanics and Mobility, Vo. 8, No. 4, pp. 187-200, 1989.
14. Cassidy, I. L., Scruggs, J. T., Behrens, S., and Gavin, H. P., "Design and Experimental Characterization of an Electromagnetic Transducer for Large-Scale Vibratory Energy Harvesting Applications," Journal of Intelligent Material Systems and Structures, Vol. 22, No. 17, pp. 2009-2024, 2011.
15. Nguyen, D. C. and Ahn, H.-J., "Semi-Active Reaction Force Compensation for a Linear Motor Motion Stage," Int. J. Precis. Eng. Manuf., Vol. 17, No. 7, pp. 857-862, 2016.
16. Ahn, H. J. and Kim, K. R., "2D Hall Sensor Array for Measuring the Position of a Magnet Matrix," Int. J. Precis. Eng. Manuf.-Green Tech., Vol. 1, No. 2, pp. 125-129, 2014.
17. Pham, M.-N. and Ahn, H.-J., "Horizontal Active Vibration Isolator (HAVI) Using Electromagnetic Planar Actuator (EPA)," Int. J. Precis. Eng. Manuf.-Green Tech., Vol. 2, No. 3, pp. 269-274, 2015.
18. Hassell, T. J., Weaver, W. W., and Oliveira, A. M., "Using Matlab's Simscape Modeling Environment as A Simulation Tool in Power Electronics and Electrical Machines Courses," Proc. of the IEEE Frontiers in Education Conference, pp. 477-483, 2013.
19. Villegas, F., Hecker, R. L., and Peña, M., "Two-State GMS-Based Friction Model for Precise Control Applications," Int. J. Precis. Eng. Manuf., Vol. 17, No. 5, pp. 553-564, 2016.